Journal of Medical Ultrasonics (2019) 46:187–194
https://doi.org/10.1007/s10396-019-00928-4

ORIGINAL ARTICLE

Identification of vascular lumen by singular value decomposition filtering on blood flow velocity distribution

Ryo Nagaoka[1] · **Hideyuki Hasegawa**[1]

Received: 20 September 2018 / Accepted: 27 December 2018 / Published online: 24 January 2019

Abstract

Purpose In the present study, we proposed a novel method for identification of the vascular lumen by employing singular value decomposition (SVD), and the feasibility of the proposed method was validated by in vivo measurement of the common carotid artery.

Method SVD filtering was applied to a velocity map that was estimated using an autocorrelation method to identify the lumen region. In this study, the packet size was set at 999 frames with a frame rate of 1302 Hz. The region estimated by the proposed SVD filtering was compared with that estimated by the conventional power Doppler method.

Result The averaged differences in feature values between vascular wall and lumen regions obtained by the proposed and conventional methods were 34 dB and 26 dB, respectively. The proposed method was hardly influenced by the cardiac phase and could separate the wall and lumen regions more stably. The proposed method could identify the lumen region by setting a threshold of − 28 dB from the averaged difference amplitude.

Conclusion We proposed a novel method for identification of the vascular lumen. The proposed method could suppress the effects of wall motion, which was present in the conventional power Doppler image. The lumen region identified by the proposed method well conformed with the anatomical information in the B-mode image of the corresponding section.

Keywords Lumen identification · Singular value decomposition filtering · Ultrasonic image · High-frame-rate imaging

Introduction

The ultrasonic measurement of blood flow is highly beneficial for diagnoses of cardiovascular diseases. Recently, high temporal resolution ultrasonic measurements using plane or diverging waves allow us to visualize the detailed dynamics of two-dimensional blood flows [1–5]. In blood flow measurements, identification of the vascular lumen is important to obtain an accurate blood flow image. For identification of the vascular lumen, several strategies have been proposed [6–10], which are based on symmetric structures of the common carotid artery (CCA) [6], statistical features of ultrasound B-mode images [7, 8], and analysis of ultrasonic RF signals [9, 10]. For cardiac applications, methods based on correlation among received ultrasonic echo signals have been developed to segment an echocardiographic image into lumen and heart wall regions [11, 12]. Also, Takahashi et al. [13, 14] and Nakahara et al. [15] improved the segmentation accuracy using an expectation–maximization (EM) algorithm.

Recently, the focus has been on singular value decomposition (SVD) filtering, with SVD filtering being applied to diagnostic modalities such as magnetic resonance imaging (MRI) [16] and X-ray computed tomography (CT) [17] to separate measured signals into desired and noise signals. In medical ultrasound imaging, SVD filtering has also been studied for the purpose of clutter reduction in blood flow measurements [18]. In our previous study [19], three different components in ultrasonic echo signals, i.e., those from tissues, blood cells, and cavitation bubbles, were separated by focusing on the difference in the spatiotemporal characteristics in high-intensity focused ultrasound (HIFU) therapy. However, an ultrasonic image could not be segmented into blood, wall, and cavitation regions by the above-mentioned method because that method just separated

✉ Ryo Nagaoka
nryo@eng.u-toyama.ac.jp

[1] Graduate School of Science and Engineering for Research, University of Toyama, 3190 Gofuku, Toyama 930-8555, Japan

ultrasonic radio-frequency (RF) signals into the respective components.

In the present study, SVD was used for identification of the blood vessel lumen in an ultrasonic image. A velocity distribution in the vascular lumen has spatiotemporal characteristics that are different from those in the blood vessel wall. Therefore, the vascular lumen could be identified by applying SVD filtering to velocity data. In the present study, we proposed a novel strategy for identification of the vascular lumen. Also, the proposed method was compared with a conventional power Doppler-based method. The proposed SVD-based filter was used for extracting a dominant spatiotemporal feature in a blood flow velocity distribution obtained by the color Doppler method. In other words, the output image from the proposed SVD-based filter in the proposed method was a component of a color Doppler image. In conventional color and power Doppler imaging, it is said that the power Doppler method is superior to the color Doppler method in terms of detection of the vessel lumen. Therefore, in the present study, the proposed method, which was used to extract a dominant spatiotemporal feature in a color Doppler image, was compared with a power Doppler image.

Materials and methods

Experimental setup

Ultrasonic echo signals were measured using the plane-wave high-frame-rate imaging sequence as described previously [20–22] with a 7.5-MHz linear array ultrasonic probe. The probe has 192 transducer elements with an element pitch of 0.2 mm. The echo signals were received with individual transducer elements, and the received signals were individually acquired using a programmable acquisition system with 96 transmit–receive channels. The sampling frequency was 31.25 MHz, corresponding to an axial step of 0.02464 mm under an assumed sound speed of 1540 m/s. In one plane-wave transmission, 24 focused receiving beams were generated at intervals of 0.2 mm by applying a delay-and-sum method to the received RF signals, and the aperture used to generate one focused receiving beam consisted of 72 elements. One image frame consisting of $24 \times 4 = 96$ focused receiving beams was obtained by four emissions of plane waves. The active aperture was shifted by 24 elements after each emission. Figure 1 shows a schematic of the transmission sequence for the high-frame-rate imaging. A pulse repetition frequency of 5208 Hz results in a frame rate of 1302 Hz. The beamformed RF signals were obtained by rectangular apodization.

Using the acquisition system described above, RF echo signals from the CCA of a 44-year-old healthy male were acquired. This study was approved by the institutional ethical committee and was performed with the informed consent of the subject.

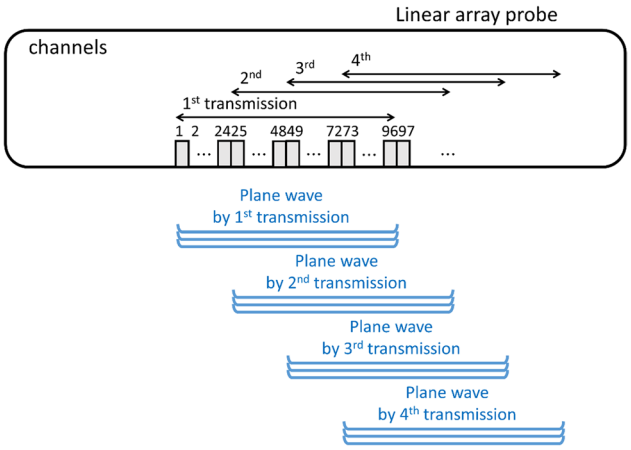

Fig. 1 Schematic of transmission sequences for high-frame-rate imaging

SVD filtering for lumen identification

SVD filtering [18, 19] was applied to an estimated velocity map to identify the lumen area. In this study, the packet size was set at 999 frames. Figure 2a, b shows flow charts of a conventional method using power Doppler and the proposed method using SVD filtering, respectively. A moving target indication (MTI) filter was applied to beamformed RF signals to suppress clutter signals, and the velocity map was then estimated using an autocorrelation method [23]. The SVD-based MTI filter proposed by Demené et al. [18] was employed in this study. The packet size for the MTI filter was set to be equal to the number used by Demené et al., i.e., 999. Also, the cutoff numbers of low and high orders selected were 65 and 850 based on a slope of the singular values [24]. The number for the low order corresponded to a boundary between components of the clutter and blood flow, and that for the high order corresponded to a boundary between components of the blood flow and noise. In the autocorrelation method, Hilbert transformation was applied to the MTI-filtered RF signals to obtain the complex autocorrelation function, which corresponded to the inner product between the resultant analytic signals in two frames. Then, velocity values were calculated from the angle of the complex autocorrelation function at a lag of zero. The lumen region estimated by the proposed SVD filtering was compared with that estimated by the conventional power Doppler method [1].

The vascular lumen was identified by applying thresholds to feature values extracted by the conventional power Doppler and proposed methods. In the conventional power Doppler-based method, the magnitude of the complex

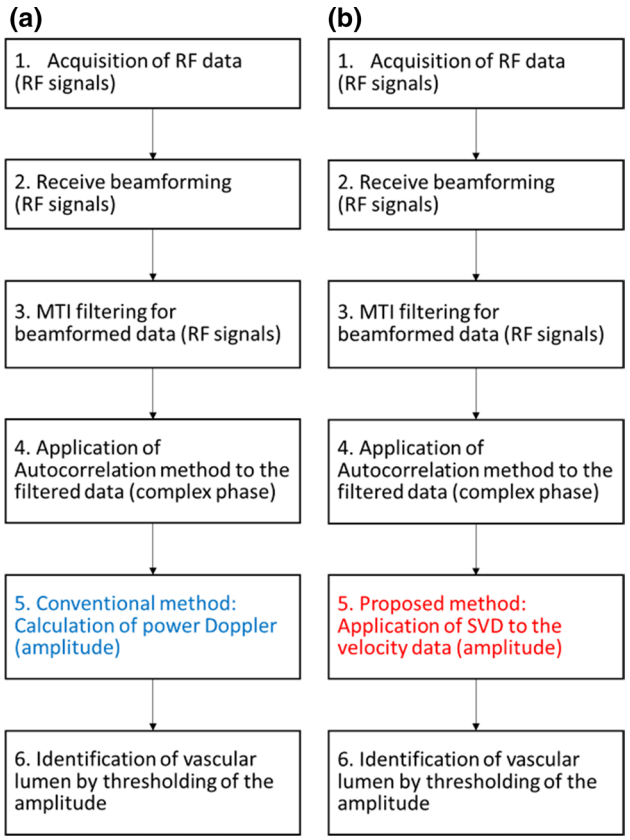

Fig. 2 Flow charts of identification strategies. **a** Conventional method using power Doppler and **b** proposed method using SVD

inner products between the analytic signals in two frames (complex autocorrelation function at a lag of zero) was used as the feature value. In the proposed method, the magnitude of blood flow velocity subjected to the proposed SVD filter was used as the feature value. By referring to the corresponding B-mode image, two regions of interest (ROIs) were set in the vascular wall and lumen to calculate feature values S_{WA} and S_{BA} in the respective regions. Then, the difference S_{DBAW} between the feature values S_{WA} and S_{BA} was employed for the comparison. The size of an ROI was 10 $\lambda \times 5$ λ in the axial and lateral directions, respectively. The feature values obtained by both methods in the successive 64 frames were averaged. In the conventional power Doppler method or color Doppler method with focused transmit beams, the estimated complex inner products between analytic signals in successive 8 or 16 packets (frames) were averaged to improve the signal-to-noise ratio (SNR). In this study, plane waves were used in transmission and, therefore, the SNR of the received ultrasonic signal was lower than that in the conventional imaging with focused beams. On the other hand, in this study, a frame rate of 1302 Hz, which was much higher than that in conventional imaging with focused beams of 20–30 Hz, was realized by plane wave imaging. Therefore, a higher number of packets (64) was used for temporal averaging.

Let us define the estimated velocity data $v(x, z, t)$, where x and z denote the lateral and axial positions, respectively. A spatiotemporal matrix $\mathbf{S}$ is created by rearranging the velocity data $v\ (x,\ z,\ t)$; $(n_x,\ n_z,\ n_t)$. To the Casorati matrix of size $(n_x \times n_z, n_t)$, where n_x, n_z, and n_t represent the number of sampling points in the lateral, depth, and frame directions, respectively. The spatiotemporal matrix $\mathbf{S}$ is decomposed into a product of three matrices by the SVD as

$$\mathbf{S} = \mathbf{U} \cdot \mathbf{\Sigma} \cdot \mathbf{V}^{\mathrm{T}}, \tag{1}$$

where $\mathbf{U}$ and $\mathbf{V}$ are the matrices consisting of spatial and temporal singular vectors, respectively. Superscript $[]^{\mathrm{T}}$ represents transpose, and $\mathbf{\Sigma}$ is a diagonal matrix composed of singular values (σ_i; $i = 0, 1, 2, \ldots, n_t - 1$) arranged in a descending order.

The SVD-filtered velocity map $\mathbf{S}^{\mathrm{f}}$ is obtained as follows:

$$\mathbf{S}^{\mathrm{f}} = \mathbf{U} \cdot \mathbf{\Sigma}^{\mathbf{f}} \cdot \mathbf{V}^{\mathrm{T}}, \tag{2}$$

where $\mathbf{\Sigma}^{\mathrm{f}}$ is a diagonal matrix whose singular values are partially set at zero. The distribution of singular values depends on the spatiotemporal features of the vessel wall and blood. The singular values were partially set at zero based on such differences in spatiotemporal features. In the present study, threshold values for the SVD filtering were chosen based on a slope of the singular values [22]. Let us define the mean squared difference α between the singular values σ_i and its number i as:

$$\alpha = \frac{1}{m_{\mathrm{e}} - m_{\mathrm{s}}} \sum_{i=m_{\mathrm{s}}}^{m_{\mathrm{e}}} \left\{\sigma_i - (a \cdot i + b)\right\}^2, \tag{3}$$

where m_{s} and m_{e} denote the start and end indexes, respectively, in the threshold process and were determined by minimizing the mean squared difference α. This process was performed from an index of 0 to $(n_t - 1)$ to separate the measured velocity map into vascular lumen and wall regions.

The velocity data were recovered from the residual singular values. The order of the singular values corresponds to the order of the energies of singular vectors in a spatiotemporal matrix because a singular value is the energy of the corresponding singular vector. A spatial and temporal vector with a higher order singular value corresponds to the higher frequency components [18]. For the reasons mentioned above, the low-order singular components are assumed to be related to the slow movements of the tissues, and thus, the velocity components related to tissue movements can be discarded by removing the low-order singular components as shown in Eq. (2). Similarly, high-order singular components are assumed to be related to rapid movements and/or random noise components in both the tissue and blood flow, and such

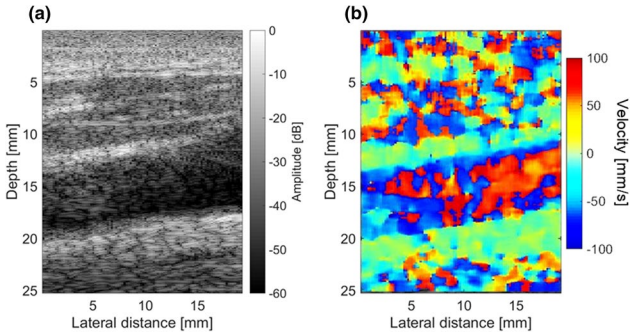

Fig. 3 **a** Conventional ultrasound B-mode image of CCA. **b** The corresponding velocity map obtained by autocorrelation method

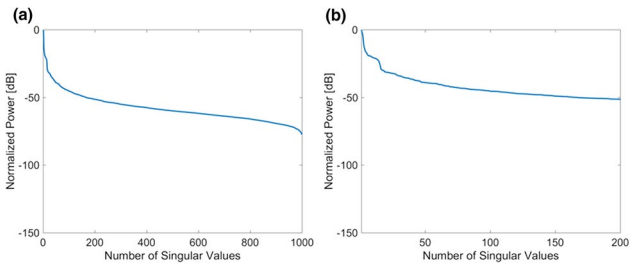

Fig. 4 Relationships between the number of singular values and the normalized power of the corresponding value in the range of **a** 1–999 and **b** 1–200

components can be suppressed by replacing higher singular values of $\mathbf{\Sigma}$ with zero.

Experimental results

Figure 3a shows a B-mode image of the CCA. By applying the autocorrelation method [23], the corresponding velocity map was obtained as shown in Fig. 3b. Figure 4 shows singular values plotted as a function of the singular value number. In Fig. 4a, b, singular values are shown in ranges of the singular value number of 1–999 and 1–200, respectively. As can be seen in Fig. 4b, there are distinct changes in slopes of the singular value distribution at a singular value number of 20. By applying the method described in Sect. 2.2, m_s and m_e were determined to be 19 and 140, respectively. As a result, the singular values in ranges of singular value numbers of 1–19 and 140–999 were set at zero.

Figure 5a shows a feature value distribution obtained by the proposed method. The proposed method clearly visualized only the lumen region. In Fig. 5a, the blue and black-dot squares correspond to the assigned vascular wall and lumen regions, respectively, to calculate the feature value difference S_{DBAW}. Figure 5b shows a distribution of feature values obtained by the conventional power Doppler method.

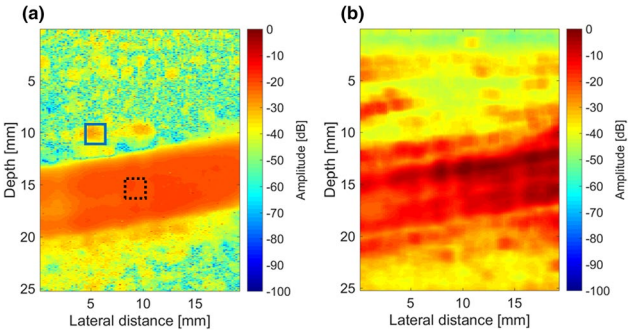

Fig. 5 Feature value distributions obtained by **a** the proposed and **b** conventional power Doppler methods

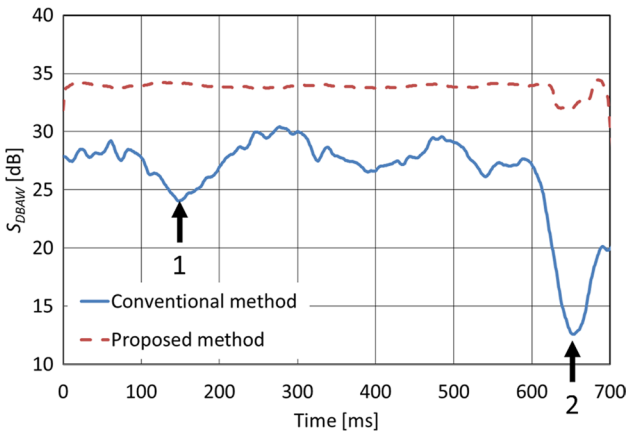

Fig. 6 Temporal changes in feature value differences S_{DBAW} obtained by the conventional power Doppler and proposed methods

Figure 6 shows temporal changes of the differences in feature values S_{DBAW} obtained by the conventional power Doppler (blue line) and proposed (red dot-line) methods. During a cardiac cycle, the average differences S_{DBAW} according to the proposed and conventional methods were 34 dB and 26 dB, respectively. The significant differences were observed at times of around 150 and 650 ms, which corresponded to end-diastolic (phase 1) and systolic (phase 2) phases, respectively. In these phases, because of the faster velocity in the vascular wall, the wall movements could not be distinguished from that of blood flow by the conventional power Doppler method. Meanwhile, the feature value difference S_{DBAW} yielded by the proposed method was constant regardless of the cardiac phase. The result indicated that the proposed method was hardly influenced by differences in phases during a cardiac cycle and could separate the feature value distribution into the wall and lumen more stably.

From these results, the region with a value of more than − 28 dB was classified as the lumen, where a threshold value of − 28 dB was determined from the above-mentioned difference S_{DBAW} during a cardiac cycle, corresponding to a

value obtained by subtracting a standard deviation from a mean value in the proposed method. Figure 7a, b shows the feature value distributions obtained by the proposed and conventional methods in phase 1, respectively. Figure 7c, d was estimated using the threshold value of −28 dB. Figure 7c, d shows lumen regions (red) identified by the proposed and conventional methods in phase 1, respectively. The blue region corresponds to the other components (including external soft tissue). Also, Fig. 8a, b shows the feature value distributions obtained by the proposed and conventional methods in phase 2, respectively. Figure 8c, d shows the identified lumen region estimated by the proposed and conventional methods in phase 2, respectively. The lumen region estimated by the conventional method included the vascular wall. On the other hand, the proposed method identified such regions as other components (vascular wall and external tissues) correctly. From these results, the proposed method was shown to identify the lumen region more accurately than the conventional method.

Also, since there was a possibility that the threshold value used above was not proper for the conventional method, Fig. 9a, b shows the lumen regions identified by the conventional power Doppler-based method at the time of 400 ms and in phase 2 (systolic phase) using a different threshold value of 21 dB, which was obtained by subtracting

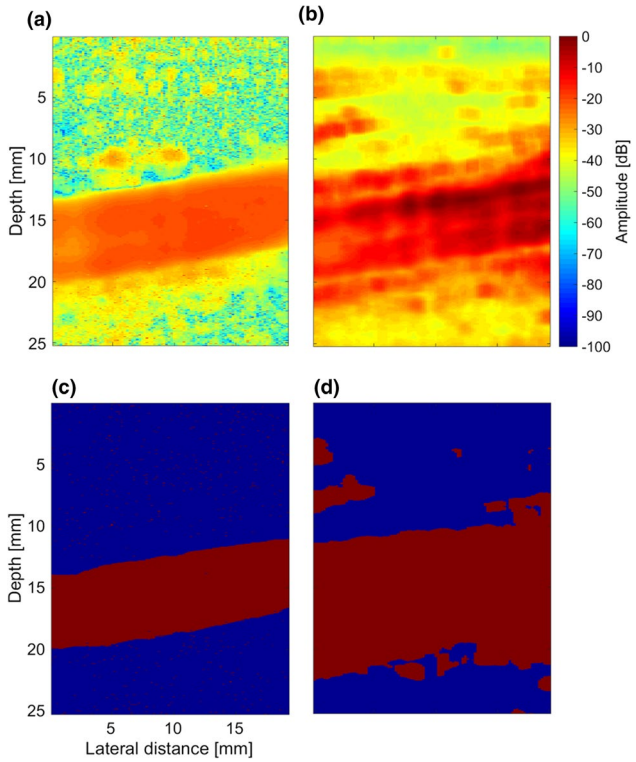

Fig. 7 Feature value distributions obtained by **a** the proposed and a conventional methods in phase 1. Lumen region identified by **c** the proposed and **d** conventional methods in phase 1

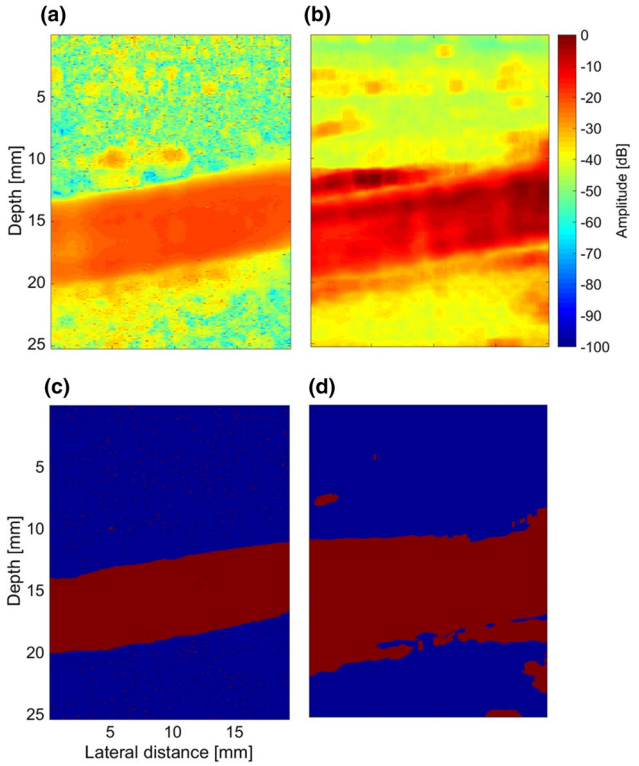

Fig. 8 Feature value distributions obtained by **a** the proposed and **b** conventional methods in phase 2. Lumen region identified by **c** the proposed and **d** conventional methods in phase 2

a standard deviation from a mean value in the conventional method. The lumen region can almost be separated from the wall region with the threshold values, as shown in Fig. 9a, because the arterial wall does not move so much at the time of 400 ms. However, the lumen region cannot be completely identified. Additionally, the lumen region cannot be separated completely from the wall region even with a lower

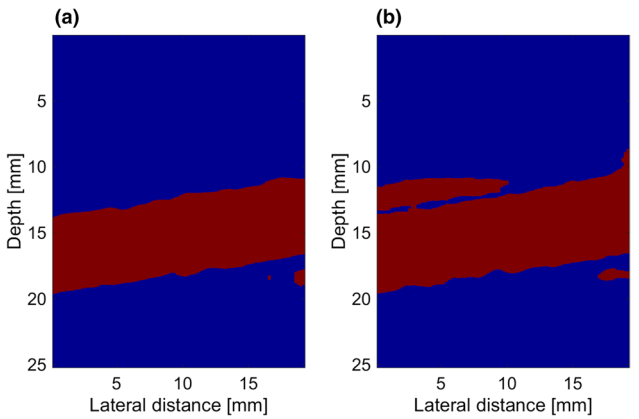

Fig. 9 Identified lumen region estimated by the conventional methods **a** at a time of 400 ms and **b** at phase 2 with a different threshold value of 21 dB

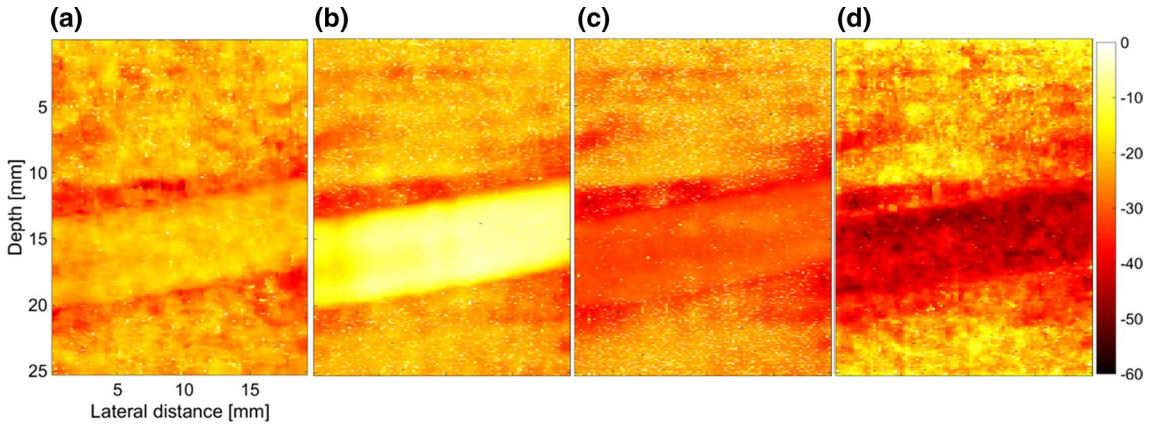

Fig. 10 Feature value distributions obtained by the proposed method with the singular values of **a** 1–19th, **b** 20–139th, **c** 140–950th, and **d** 951–999th

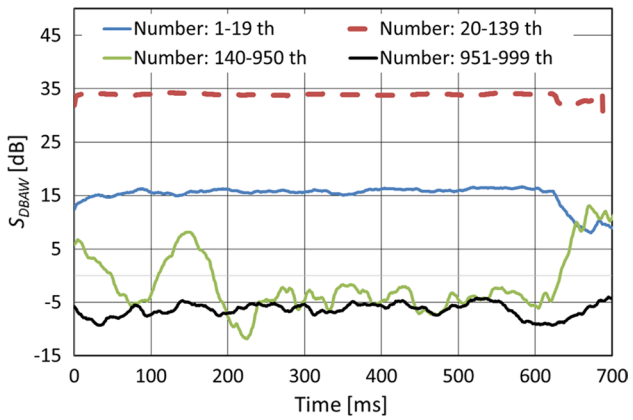

Fig. 11 Temporal changes in feature value difference S_{DBAW} in the same region as that shown in Fig. 5 with the different singular value range

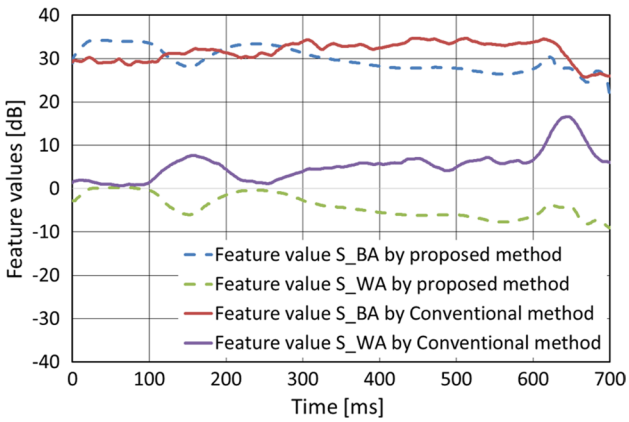

Fig. 12 Feature values S_{BA} and S_{WA} obtained by the conventional power Doppler and proposed methods

threshold value because the wall region rapidly moves in phase 2 (systolic phase).

Discussion

Principal component of each singular value

In this study, the lumen region was identified by replacing 1–19th and 140–999th of 999 singular values with zero. Based on the slope of the singular value distribution, the components of estimated velocities could be categorized into four groups. Figure 10 shows the feature value distributions corresponding to the singular values of (a) 1–19th, (b) 20–139th, (c) 140–950th, and (d) 951–999th. Also, Fig. 11 shows the temporal changes of feature value differences S_{DBAW} in the same region as shown in Fig. 5 with the corresponding singular value ranges. The components in Fig. 10a, d correspond to the slower movements in the soft tissue and the noise, respectively. According to these results, the feature value difference S_{DBAW} of the 20–139th singular values identifies the lumen region most stably, and the singular values in that range of the singular value numbers correspond to the velocity components of the flow velocity in the lumen region.

In Fig. 6, a difference between feature values S_{DBAW}, which is stable during a cardiac cycle, can be obtained by the proposed method, while S_{DBAW} obtained by the conventional power Doppler image shows some fluctuations. There are mainly two cardiac phases, i.e., cardiac ejection phase and aortic valve closure phase, in which feature values S_{BA} and S_{WA} fluctuate. Figure 12 shows temporal changes of feature values S_{BA} (lumen region) and S_{WA} (wall region) obtained by the conventional power Doppler and proposed methods. Basically, the output of the power Doppler method corresponds to the amplitude of the MTI-filtered (high-pass filtered) ultrasonic echo. In the cardiac ejection phase and

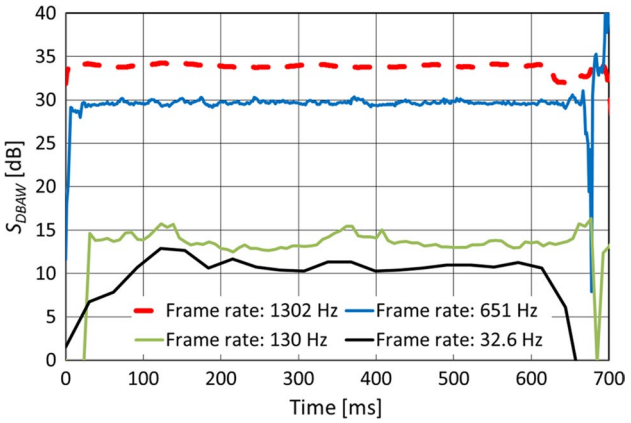

Fig. 13 Temporal changes in amplitude difference S_{DBAW} in the same region as that shown in Fig. 5 with the different frame rates

aortic valve closure phase, the arterial wall moves rapidly. Therefore, high-pass filtered ultrasonic echoes from the arterial wall increase, which leads to the increases in the feature values S_{WA} in those phases obtained by the power Doppler method.

On the other hand, the proposed method is considered to have a band-pass characteristic, and the cutoff boundaries for higher and lower order singular values, which correspond to noise and tissue, respectively, are determined adaptively. The rapid changes in the velocity distributions in the cardiac ejection phase and aortic valve closure phase were considered to cause changes in such cutoff characteristics. As a result, some velocity components in rapidly varying blood flow were possibly recognized as noise, and some velocity components in the fast-moving arterial wall were possibly considered as blood flow. Therefore, both S_{BA} for blood flow and S_{WA} for the arterial wall decreases in those two phases, and thus, the difference between them was considered not to fluctuate even in those phases.

Effects from difference in imaging frame rates

The influence of the imaging frame rate was investigated by decimating the frames by factors n of 1 (1302 Hz), 2 (651 Hz), 10 (130 Hz), and 40 (32.6 Hz). Figure 13 shows the temporal changes of amplitude differences S_{DBAW} in the same regions shown in Fig. 5 at different frame rates. By decreasing the frame rate, the difference S_{DBAW} decreased and was more affected by the phases during a cardiac cycle. Consequently, the proposed method prefers a high frame rate. In the case of measurement of the carotid artery, an imaging frame rate of more than 1302 Hz would be preferable. This is because the temporal continuity of speckles in the estimated blood flow velocity map declines with the decrease in the frame rate.

Conclusions

In the present study, we proposed a novel method for identification of the vascular lumen. Also, the result was compared with that obtained using a conventional power Doppler method. SVD filtering was applied to the estimated velocity map to identify the lumen area. During one cardiac cycle, the averaged feature value differences S_{DBAW} obtained by the proposed and conventional methods were 34 dB, and 26 dB, respectively. The proposed method was hardly affected by cardiac phases and could separate the estimated velocity distribution into the wall and lumen regions much more accurately. The proposed method has been shown to be less influenced by wall motion, which often causes problems in segmentation using a conventional power Doppler image. The lumen area identified by the proposed method well conformed to the anatomical information in the B-mode image of the corresponding section.

Acknowledgements This work was supported by JSPS Grant-in-Aids for Early-Career Scientists 18K18395 and Scientific Research (B) 17H03276.

Compliance with ethical standards

Ethical considerations This study was approved by the institutional ethical committee and was performed with the informed consent of the subject.

Conflict of interest The author(s) declare that they have no competing interests.

References

1. Yiu BYS, Lai SSM, Yu ACH, et al. Vector projectile imaging: time-resolved dynamic visualization of complex flow patterns. Ultrasound Med Biol. 2014;40:2295–309.
2. Takahashi H, Hasegawa H, Kanai H. Echo speckle imaging of blood particles with high-frame-rate echocardiography. Jpn J Appl Phys. 2014;53:1–7.
3. Takahashi H, Hasegawa H, Kanai H. Echo motion imaging with adaptive clutter filter for assessment of cardiac blood flow. Jpn J Appl Phys. 2015;54:1–8.
4. Takahashi H, Hasegawa H, Kanai H. Temporal averaging of two-dimensional correlation functions for velocity vector imaging of cardiac blood flow. J Med Ultrason. 2015;42:323–30.
5. Fadnes S, Bjærum S, Torp H, et al. Clutter filtering influence on blood velocity estimation using speckle tracking. IEEE Trans Ultrason Ferroelectr Freq Control. 2015;62:2079–91.
6. Rouco J, Azevedo E, Campilho A. Automatic lumen detection on longitudinal ultrasound b-mode images of the carotid using phase symmetry. Sensors. 2016;16:1–21.
7. Santos AMF, Tavares JMRS, Souca L, et al. Automatic segmentation of the lumen of the carotid artery in ultrasound B-mode images. Conf Proc in SPIE Med Imge. 2013;8670:1–16.

8. Mendizabal-Ruiz G, Rivera M, Kakadiaris IA. A probabilistic segmentation method for the identification of luminal borders in intravascular ultrasound images. In: Proc in 2008 IEEE Conf. on computer vision and pattern recognition. 2008;53:pp 1–4.
9. Ibrahim N, Hasegawa H, Kanai H. Detection of boundaries of carotid arterial wall by analyzing ultrasonic RF signals. Jpn J Appl Phys. 2012;51:1–8.
10. Ibrahim N, Hasegawa H, Kanai H. Detection of arterial wall boundaries using an echo model composed of multiple ultrasonic pulses. Jpn J Appl Phys. 2013;51:1–10.
11. Kinugawa T, Hasegawa T, Kanai H. Automated segmentation of heart wall using coherence among ultrasonic RF echoes". Jpn J Appl Phys. 2008;47:4155–64.
12. Nillesen MM, Lopata RGP, Huisman HJ, Thijssen JM, Kapusta L, de Korte CL. Correlation based 3-D segmentation of the left ventricle in pediatric echocardiographic images using radio-frequency data. Ultrasound Med Biol. 2011;37:1409–20.
13. Takahashi H, Hasegawa H, Kanai H. Automated identification of the heart wall throughout the entire cardiac cycle using optimal cardiac phase for extracted freatures. Jpn J Appl Phys. 2011;50:1–9.
14. Takahashi H, Hasegawa H, Kanai H. Improvement of automated identification of the heart wall in echocardiography by suppressing clutter component. Jpn J Appl Phys. 2013;50:1–7.
15. Nakahara K, Hasegawa H, Kanai H. Optimization of feature extraction for automated identification of heart wall regions in different cross sections. Jpn J Appl Phys. 2014;50:1–9.
16. Otazo R, Candes E, Soldickson DK, et al. Low-rank and sparse matrix decomposition for accelerated dynamics MRI with separation of background and dynamic domponetns. Magn Reson Med. 2014;73:1125–36.
17. Gao H, Yu H, Osher S, et al. Multi-energy CT based on a prior rank, intensity and sparsity model (PRISM). Inverse Probl. 2011;27:1–30.
18. Demené C, Deffieux T, Pernot M, et al. Spatiotemporal clutter filtering of ultrafast ultrasound data highly increases doppler and ultrasound sensitivitiy. IEEE Trans Med Image. 2015;34:2271–85.
19. Ikeda H, Nagaoka R, Lafond M, et al. Singular value decomposition of received ultrasound signal for separation among tissue, blood flow and cavitation signals. Jpn J Appl Phys. 2018;57:1–6.
20. Hasegawa H, Kanai H. Simultaneous imaging of artery-wall strain and blood flow by high frame rate acquisition of RF signals. IEEE Trans Ultrason Ferroelectr Freq Control. 2008;55:2626–39.
21. Hasegawa H. Improvement of penetration of modified amplitude and phase estimation beamformer. J Med Ultrason. 2017;44:3–11.
22. Hasegawa H. Apodized adaptive beamformer. J Med Ultrason. 2017;44:155–65.
23. Kasai C, Namekawa K, Koyano A, et al. Real-Time Two-Dimensional Blood Flow Imaging Using an Autocorrelation Technique. IEEE Trans Sonics Ultrason. 1985;32:458–64.
24. Song H, Trzasko JD, Manduca A, et al. Accelerated singular value-based ultrasound blood flow clutter filtering with randomized singular value decomposition and randomized spatial downsanpling. IEEE Trans Ultrason Ferroelectr Freq Control. 2017;64:706–16.